Raman water vapor lidar calibration

E. Landulfo[a], R. F. Da Costa[a], A. S. Torres[a], F.J.S. Lopes[a], D. N. Whiteman[b], D. D. Venable[c]

[a]Instituto de Pesquisas Energéticas e Nucleares, Av. Prof. Lineu Prestes 2242,05508-000, São Paulo, Brazil; [b]NASA - Goddard Space Flight Ctr., Building 33, Greenbelt, MD, USA, 20771; [c]Howard University, 2400 Sixth Street, NW, Washington, DC, USA, 20059;

ABSTRACT

We show here new results of a Raman LIDAR calibration methodology effort putting emphasis in the assessment of the cross-section ratio between water vapor and nitrogen by the use of a calibrated NIST traceable tungsten lamp. Therein we give a step by step procedure of how to employ such equipment by means of a mapping/scanning procedure over the receiving optics of a water vapor Raman LIDAR. This methodology has been independently used at Howard University Raman LIDAR and at IPEN Raman LIDAR what strongly supports its reproducibility and points towards an independently calibration methodology to be carried on within an experiment routine.

Keywords: LIDAR, Raman LIDAR, Calibration, Water Vapor

1. INTRODUCTION

It is already known that the Raman Lidar is a well established technique for atmospheric measurements and also for atmospheric species concentration determination.[1] In the case of the water vapor mixing ratio determination we need to know the backscattering Raman signal from water vapor and nitrogen or oxygen as reference gases. Moreover in order to get reliability in the measurement and accuracy assessment the Raman Lidar system should go through a calibration process analysis. The first documented effort to perform a system calibration was made by Vaughan et al.[2] by the determination of the relative instrumental transmission defined as the product of the transmission of the filter, the transmission of the collimating optics, the beamsplitter efficiency and the quantum efficiency of the photodetector used in that work and the Raman cross section ratio. After some assumptions Vaughan et al. considered the only unknown, apart from the water vapor mixing itself, the cross section ratio between the water vapor and nitrogen as reference gas, which was taken from laboratory measurements made by Penney and Lapp[3] or Lidar observations themselves.[4] In that effort the error estimation for the water vapor mixing ratio was claimed as being $\approx 12\%$. The next calibration work was made about a decade later by Sherlock et al.[5] In that work they reposed their method on the decomposition of the instrument function which allowed the calibration coefficient to be expressed as the product of the instrumental transmission combined with detection efficiency and the wavelength dependent convolution of the Raman backscatter cross sections with the system instrumental function. In order to verify their instrument response they used for calibration two light source types: the zenith observation of diffuse sunlight and a xenon arc lamp. A general quantum mechanical model was chosen for the determination of the cross sections involved in the calibration process. In their study they claimed a total error budget of 10-14%. However, they claimed that the changes of the calibration factor in a long term basis were less than 9%. More recently many studies related to a Raman lidar calibration method were published related to alternative methods,[6] geographical extensivity[7] or to check the process long-term feasibility.[8, 9] In our calibration methodology which started at Howard University, Beltsville Campus[10] following up a seminal work by Whiteman et al.[11] we have been looking for a smaller uncertainty and an independent procedure to calibrate a Raman Lidar system for water vapor measurements. In this approach we verified a Raman Lidar system spectral response which is located at the Environment Laser Applications Laboratory at the Center for Laser and Applications at IPEN/CNEN, São Paulo, Brazil, designed to make nighttime measurements of atmospheric water vapor and aerosols. This spectral response analysis was carried on with a calibrated light source which we had to check its emissivity pattern according to the Planck's law and cross-check with the manufacturer referred

Further author information: (Send correspondence to Eduardo Landulfo)
E-mail: elandulf@ipen.br, Telephone: +55 11 3133 9372

data. Following our procedure we have performed a geometrical scan over the MSP Raman Lidar (MSPRL) telescope system, thus verifying its response homogeneity and relative efficiency of nitrogen over water vapor channels. In this first phase of our methodology we used a set of interference filters in front of the MSPRL system detectors in order to obtain the cross section ratio between the water vapor and nitrogen following a convolution of the filter transmission curves with the spectral irradiance of the calibrated lamp within a given spectral interval. In the whole process described in the methodology we should give the details of this procedure and in the results come up with a experimentally estimate of the cross section ratio. Our preliminary results pointed out to a cross section ratio $((d\sigma_N/d\Omega)/(d\sigma_H/d\Omega))$ in fairly good agreement with those given in the literature so far.[3, 5, 12–14] The next step or phase of our methodology should carry the same procedure with a narrower band set of filters and thus find an expected long-term valid calibration factor for routine water vapor Raman Lidar measurements provided the whole experimental set stays the same. This last phase should be discussed elsewhere and in future experiments to be carried on.

2. METHODOLOGY

The water-vapor mixing ratio, ω, is a convenient measure of the amount of water vapor in the atmosphere and is given by the ratio of the mass of water vapor to the mass of dry air in a given volume. From traditional Raman Lidar Equation[1] the ratio of the single-scattering Raman Lidar measurements of water vapor (H) and nitrogen (N) can be represented[1] as:

$$\frac{P(\Delta\lambda_H, r)}{P(\Delta\lambda_N, r)} = \frac{O_H(r)F_H[T(r)]N_H(r)[d\sigma_H(\lambda_L, \pi)/d\Omega]\xi(\lambda_H)}{O_N(r)F_N[T(r)]N_N(r)[d\sigma_N(\lambda_L, \pi)/d\Omega]\xi(\lambda_N)} \exp\left\{ -\int_0^r [\alpha(\lambda_H, r') - \alpha(\lambda_N, r')dr'] \right\} \quad (1)$$

where $P(\Delta\lambda_X, r)$ is the backscattered power (after any background contribution that is due, for example, to skylight or detector noise, is subtracted) received at wavelength λ_X as a function of range, r. $O_X(r)$ is the overlap function for channel X, $\xi(\lambda_X)$ is the optical efficiency of the system, $N_X(r)$ is the number density of molecular species X that is being excited, and $d\sigma_H(\lambda_L, \pi)/d\Omega$ is the pertinent Raman backscatter cross section. The atmospheric transmission function includes a term α at the laser wavelength λ_L, for the transmission along the output path and another for the backscattered signal at the wavelength λ_X, that has been shifted from the laser wavelength owing to inelastic Raman scattering by molecular species X. $F_X[T(r)]$ is the term that describes the temperature dependence of vibrationalrotational scattering on the Raman Lidar equations.[1, 12]

The water-vapor mixing ratio equation can now be expressed by use of a single calibration factor as follows:

$$\omega = k^*(r)\frac{F_N[T(r)]P(\Delta\lambda_H, r)}{F_H[T(r)]P(\Delta\lambda_N, r)} \exp\left\{ -\int_0^r [\alpha(\lambda_H, r') - \alpha(\lambda_N, r')dr'] \right\} \quad (2)$$

where $k^*(r)$ is the lidar systems calibration factor, represented by

$$k^*(r) \cong 0.485\frac{O_N(r)[d\sigma_N(\lambda_L, \pi)/d\Omega]\xi(\lambda_N)}{O_H(r)[d\sigma_H(\lambda_L, \pi)/d\Omega]\xi(\lambda_H)} \quad (3)$$

In order to calculate the $k^*(r)$ factor, we estimated the total efficiency ratio and the Raman cross section ratio by a experimental procedure showed in detail bellow.

The response or *detection* efficiency can be defined by the convolution of the Planck emission of a calibrated light source by the filter spectral response at a given detection channel bandwidth :

$$\xi'(\lambda_X) = \int_{\lambda_{X_1}}^{\lambda_{X_2}} W(\lambda_X) \times \zeta(\lambda_X)d\lambda_X \quad (4)$$

where W is the emissivity blackbody Planck function and $\zeta(\lambda_X)$ is the response(detection) filter function at the bandwidth, $\Delta\lambda_X = \lambda_{X_2} - \lambda_{X_1}$. In other hand, a system optical efficiency is simply given by the ratio of the output intensity signal or response by the incident intensity, therefore in our case:

$$\xi(\lambda_X) = \frac{I_{out}(\lambda_X)}{I_{in}(\lambda_X)} \tag{5}$$

If then we take the ratio of the nitrogen channel by the water vapor one we get to:

$$\frac{\xi(\lambda_N)}{\xi(\lambda_H)} = \frac{I_{out}(\lambda_N) \times I_{in}(\lambda_H)}{I_{out}(\lambda_H) \times I_{in}(\lambda_N)} \tag{6}$$

and as $I_{out}(X) = \xi'(\lambda_X)$:

$$\frac{\xi(\lambda_N)}{\xi(\lambda_H)} = \frac{\xi'(\lambda_N)}{\xi'(\lambda_H)} \times \frac{I_{in}(\lambda_H)}{I_{in}(\lambda_N)} \tag{7}$$

Finally, by combining 7 with 4:

$$\frac{\xi(\lambda_N)}{\xi(\lambda_H)} = \frac{\int_{\lambda_N-\Delta_{\lambda_N}}^{\lambda_N+\Delta_{\lambda_N}} W(\lambda_N) \times \zeta(\lambda_N) d\lambda_N}{\int_{\lambda_H-\Delta_{\lambda_H}}^{\lambda_H+\Delta_{\lambda_H}} W(\lambda_H) \times \zeta(\lambda_H) d\lambda_H} \times \frac{I_{in}(\lambda_H)}{I_{in}(\lambda_N)} \tag{8}$$

Here Δ_{λ_X} is the filter centroid difference to its own edges, determined not by the FWHM, but to an extension where the filter sensitivity is above given value in a way that the overall area under the filter curve does not change by more than 0.5%. The filter curves were supplied their manufactures and cross checked at IPEN's spectrometry facilities. Also $I_{in}(\lambda_X)$ are count rate at each channel during the mapping/scanning procedure.

For our experiment $W(\lambda_X)$ is the spectral irradiance from a calibration lamp, namely a 1000-Watt quartz halogen tungsten coiled-coil filament lamp (S-990 Optronic), extrapolated from a Planck function curve corresponding to the interference filter wavelengths interval, times a filter correction factor $\zeta(\lambda_X)$, which also might be multiplied by the transmission "window" profile of one or more interference/neutral density filters employed for linearity correction purposes.[12]

The Tungsten lamp irradiance $W(\lambda)$ can be fitted to a Planck function defined as:

$$W_\lambda = \frac{c_2}{\lambda^5(e^{c_1/\lambda T} - 1)} \tag{9}$$

Where c_1 e c_2 are constants derived from the speed of light, Planck and Boltzmann constants.

In order to obtain $I_{out}(\lambda_X)$, a measurement of the count rate in function of the lamp position over the telescope aperture, called mapping, was performed. When scanning the telescope portions of the telescope will be illuminated that correspond to the far field collection area of the primary mirror and after passing the field stop will reach the "detector" section of the system, in other words in order to perform a complete areal analysis of the efficiency of the lidar system the telescope should be scanned in its entire aperture. The integration time was estimated to be 10s, based on the recording time of the system for a given set of interference filters and overall count rate in each channel. To estimate the Raman cross section ratio without the temperature dependence a set of filters should have a combination of passband and wavelength centroid which will guarantee a weak sensivity to temperature changes.[1] In the case of the water vapor this is more critical that in the case diatomical molecules such as O_2 and N_2. To complete this evaluation one should carry a regular water vapor mixing ratio measurement with the Lidar system and compared with a profile obtained by an external instrument such as a radiosonde. In our case it was taken from the meteorological service SBMT Marte Civ Observation center which is about 10 km from the Lidar station. In that fashion we were able to determine the $k^*(r)$ factor from equation 3 by isolating the cross section ratio term.

The MSP Raman Lidar (MSPRL) system, used in this calibration effort, is located in a suburban area in the city of São Paulo (23°33" S, 46°44" W) and was designed to make nighttime measurements of atmospheric water vapor and aerosols. The three-channel lidar system's laser operates at the third harmonic of Nd:YAG. The Lidar uses narrow band pass filters to measure the elastic backscattered and the pure rotational Raman signals at 354.7 nm, the Raman scattered photons from nitrogen molecules at 386.7 nm, and the Raman scattered photons from water vapor molecules at 407.5 nm. The set of filters employed was:

Table 1. Filter Features for the WV Raman cross section determination

λ_0	$\Delta\lambda$
389.17 nm	23.34 nm
408.51 nm	17.68 nm

As noted the filter widths are large enough to eliminate temperature dependences it might appear, however as it will be later discussed there is about 14% overlap between their contours which should be taken into account to evaluate the cross section ratio.

3. RESULTS

3.1 Lamp Characterization

Based on the spectral irradiance of a blackbody defined by the Planck's radiation law, a tungsten lamp was used for the calibration setup: the system transmission efficiency. The assigned values of total irradiance for each wavelength were extracted from the manufacturer's handbook and bear uncertainties of ±1%. However, a study was performed to confirm the blackbody behaviour of the lamp. Instead we observed that the tungsten lamp has, in fact, a *quasi-blackbody* behaviour because the Planck function does not fit the nominal spectral irradiance over all spectral range following the lamp's manufacturer values. An 8th order polynomial function was fitted to the tungsten Lamp instead as depicted by Figure 1.

3.2 Telescope Mapping

A mapping of the telescope aperture was performed changing the tungsten lamp position to evaluate the homogeneity detector response. The mapping describes the count rate over the primary mirror and light intercepting areas of the telescope. To move the lamp over the mapping area there was an ensemble with a motorized programmable translation stage. The first step in this part of the calibration process was to create a n-square matrix in which each cell had a x and y coordinate, namely $c_{x_n y_n}$. Each cell is evenly spaced so a straightforward coordinate versus cell number correspondence could be established. After some test runs we came up with a 12×12 matrix configuration which should be scanned cell by cell and register in each of them the count rate in photoncounting mode with a transient recorder in two channels: H_2O and N_2. After that we have evaluated the ratio of this two channels and ended up with 144 elements. As seen by Figure 2 we have a "sensitive" area where the count rate is above a certain threshold to be considered as part of the telescope effective area. From this selection of cells, the effective ratio or $\frac{I_{in}(\lambda_H)}{I_{in}(\lambda_N)}$, is the one that excludes the border areas and the telescope central region where the secondary mirror mounting is placed and therefore an obstructing optical element to the primary mirror, so the selected cells were those which beared a certain amount of counts were representative of those areas not influenced by any obstructions or close to a mechanical edged and after this selection was made an average was considered to be included in the final calculation. An important remark to be made is that in order to have both channels operating under a linear regime[12] we had to put in front of each detector (photomultiplier modules) a neutral density filter to bring down the photon count rate to correct for photon pileup effects and should be around 20 MHz. In effect this brings a new term to equation 8:

$$\frac{\xi(\lambda_N)}{\xi(\lambda_H)} = ❶ \times ❷ \times ③ \tag{10}$$

Where ❶ and ❷ correspond to the two previous terms in equation 8 and ③ is a transmission like term from the neutral density filter used in this experiment, namely $OD = 2.0$ or $T \approx 0.023$. In fact this will play an ultimate role in the cross section evaluation.
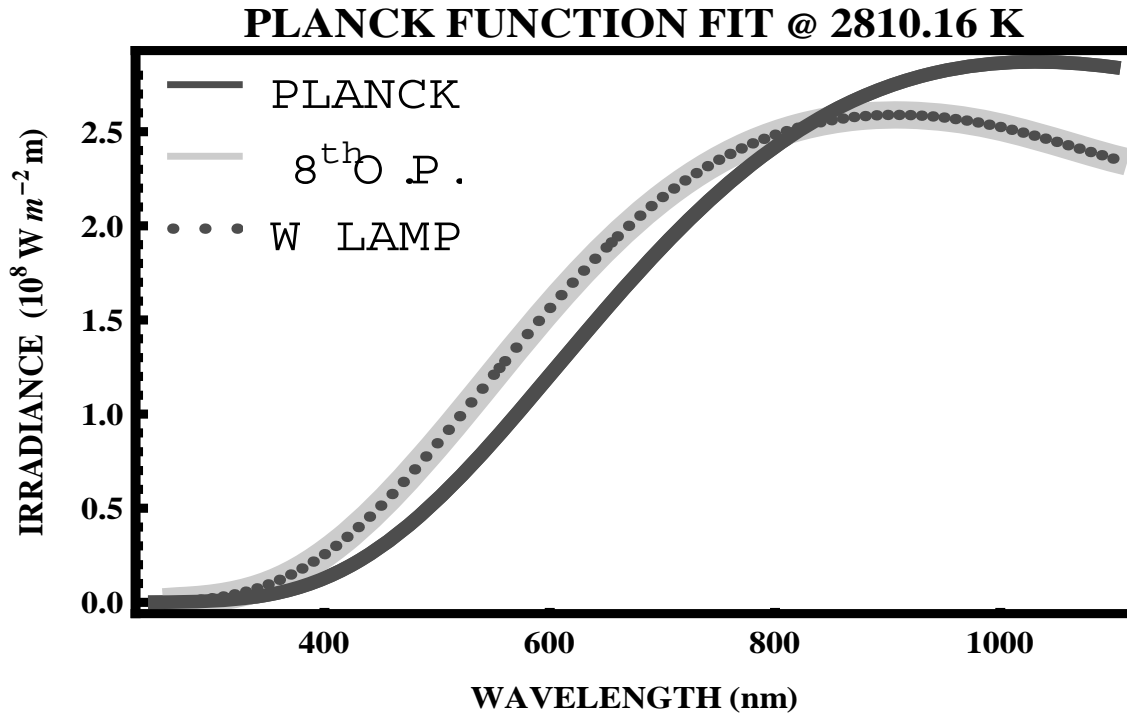
PLANCK FUNCTION FIT @ 2810.16 K

Figure 1. Irradiance fitting to the tungsten lamp employed in the calibration procedure. The lamp nominal working temperature was found as 2810.16 K. It is clear to observe that the Planck function does not match the manufacture's values over the entire spectral range and therefore an 8th order polynomial was applied instead.

Finally for the mapping run we got an average channel ratio of $(0.071 \pm 0.004)^{-1}$ (❷). Note that the equation second term after the rearrangements reads λ_H/λ_N therefore the inverse of the value above should be considered.

3.3 Lamp - Filter Function Convolution

Figure 3 shows an overview of the convolution described in equation 8. There it can be seen the Planck function $W(\lambda_X)$, $\zeta(\lambda_X)$ filter function for each channel and the ND transmission curve. The plot is given in arbitrary units but provides us a nice idea of the convolution resulting areas (dark shaded). As mentioned before an interesting remark lies on the "unwanted" overlap between the two resulting curves due the large filter bandwidths. This will generate 2 important corrections:

- The ratios considered in equation 8 should be evaluated taking into account that this overlap should be subtracted from either channel and added into another in order to retrieve the channel ratio.

- For the Lidar measurement that will use these filters a cross-talk factor should be also included considering that the counts partially recorded from one channel in fact belongs to the other and given the total cross section of the N_2 being larger that the one for H_2O we reduced the former signal accordingly.

One other point to bring under discussion is that the ND curve was transmission was taken as a constant value of 0.023 (③) under the two filter spectral range and in the case of Figure 3 it might be somehow misleading as arbitrary units were employed in that plot but in fact this mean value could be taken as a basic statistical analysis shows that the mean and median transmission values are less than 1% apart, so in other words the curve shape of the ND given in figure 3 might give the impression that a rather variable behaviour might be playing a distinctive role in defining the final convoluted curves which in fact is not. After all these considerations the value found for the convolution ratio was 0.545 ± 0.002 (❶).
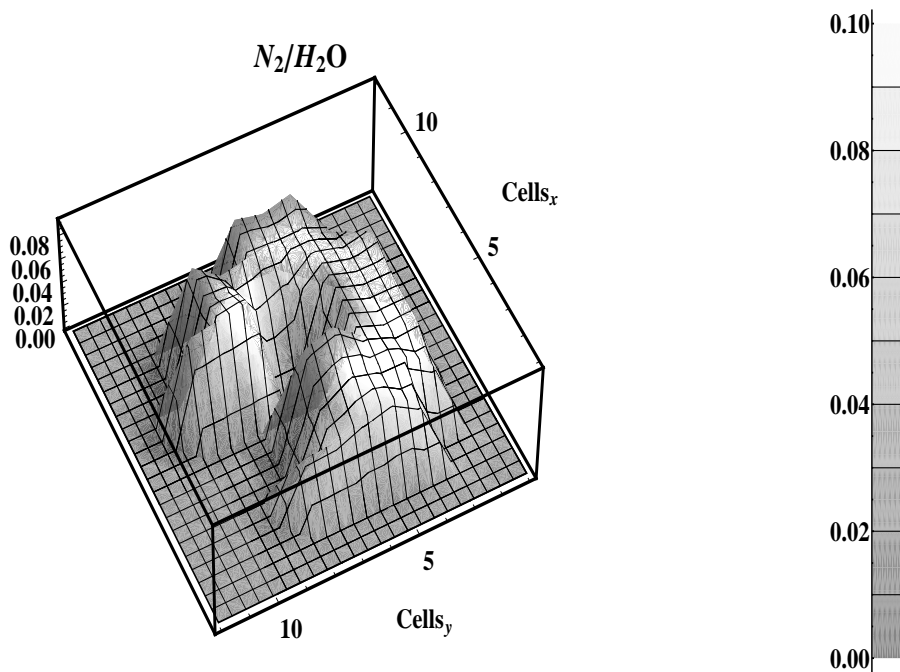
Figure 2. Mapping with a tungsten lamp over the telescope area. The 12×12 was defined after some test runs and describes a cartesian $(x \times y)$ areal coverage of the effective detection area over the telescope primary mirror aperture. The results shown here correspond to the average channel ratio of each cell.
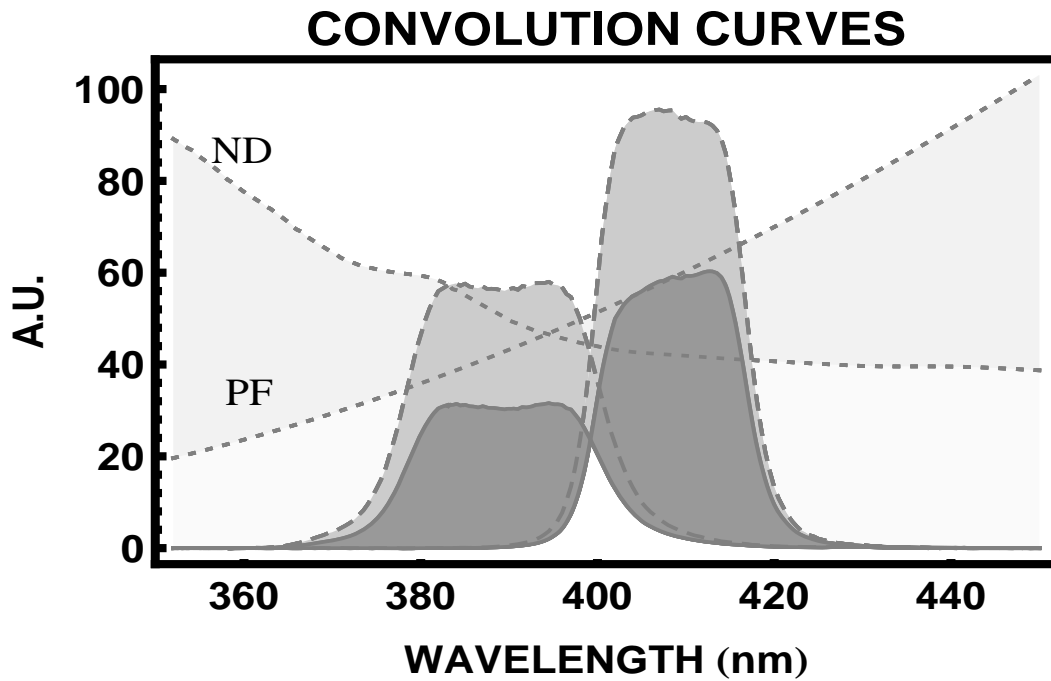

Figure 3. Convolution plot (dark shaded area) of the tungsten lamp(PF), filter functions and ND transmission curve. Arbitrary units were employed. The overlap between the convolved curves represent about 14% of the summed areas.

3.4 Raman cross section ratio evaluation

Up to date a theoretical model implemented by Avila et al[13] has been used to calculate the water vapor Raman cross sections with good accuracy.[1] For the nitrogen Raman cross sections, the calculation is also well established and fully used in Lidar science.[15] Instead, in this experiment we have performed an "experimental" cross section evaluation with the goal of not having temperature dependence with the Raman cross sections, and describing the system reception characteristics. By comparing the Raman Lidar water vapor mixing ratio profile obtained using a wide band configuration, with a radiosonde launched from a weather service station around the time of measurement and located NW of the Lidar site we were able to estimate a calibration factor $k^*(r)$ (Figure 4) and by isolating the cross section ratio in equation 3 we estimate an experimental value of this ratio, useful to calculate our Lidar independent calibration factor. Figure 4 presents the comparison profile of water vapor mixing ratio from a Lidar and from the radiosonde profile data whithin 1200 m and 2400 m where it is guaranteed to have a Lidar overlap factor close to unity.
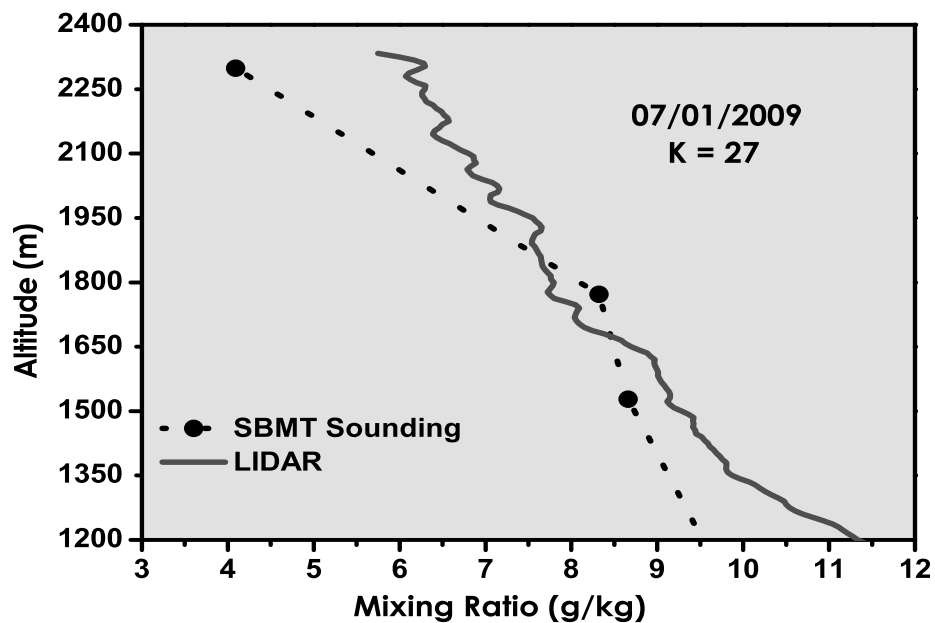

Figure 4. Water vapor mixing ratio from Raman Lidar and radiosonde data taken on 01 July 2009. We found a calibration factor k^* of 27 to be used in the cross section ratio evaluation.

Due the fact the radiosonde is about 10 km apart from the Lidar site we might get discrepancies as different parts of the atmosphere are being probed by the two instruments. From the data taken on 1 July 2009 we got a constant factor $k^* = 27$ for an altitude range mentioned previously. By isolating cross sections ratio above and using Overlap ratio equal 1, and the overall efficiency obtained through the lamp mapping and convolution curves: ❶ × ❷ × ③ = 0.177 ± 0.006. Thus the cross section ratio value obtained by this experiment was:

$$\frac{d\sigma_N(\pi)/d\Omega}{d\sigma_H(\pi)/d\Omega} = 0.32 \pm 0.04$$

After Table 2 which shows the literature values we are in fairly good agreement, remembering that some of our experimental setup features could be improved or optimized. The values shown in that table are from experimental and model evaluations, earlier papers use the inverse ratio as considered in this paper and are shown where available and with the number of most significant digits given accordingly to reflect the accuracy involved in the experimental setup.

Table 2. Typical values of the Raman cross sections ratio at branch Q, from literature, theoretical and experimental approaches.

λ_0	$(d\sigma_N/d\Omega)/$ $(d\sigma_H/d\Omega)$	References
514 nm	0.49 ± 0.05	Sherlock et al., 1999[5]
337.1 nm	0.36 or $(2.8)^{-1}$	Measures, 1984[14]
514.5 nm	0.40 ± 0.04 or $(2.5 \pm 10\%)^{-1}$	Penney and Lapp, 1976[3]
354.7 nm	0.3957	Calculated from Avila's[13] model for H_2O and Weitkamp[15] for N_2
354.7nm	0.32 ± 0.04	This experiment $k^* = 27$ and ❶ × ❷ × ③ $= 0.177 \pm 0.006$

4. CONCLUSIONS

In this methodology we present the first steps towards an independent water vapor Raman Lidar calibration by the use of a calibration source, namely a tungsten lamp and from first principles considering the convolution of optical components and detection effeciency curves. The main goal achieved was to obtain an experimental cross section ratio from measurements made using wide band interference filters on the reception system to avoid temperature dependence system response. This cross section ratio, in our case, describes the system response for Raman cross sections within the spectral interval given by the interference filters. The procedure also involved a scanning process over the aperture of telescope the primary mirror again to evaluate the system detection efficiency and optical areal response homogeinity. This involved the use of neutral density filters which should be taken into account in the cross section evaluation. Also due bandwidth overlap of the filter employed further corrections should be carried on. The final step of this experiment involved a "real" measurement of the water vapor profile in concomitance with a radiosonde launch from a nearby weather service station which achieved the final value of the cross section ratio as 0.32 ± 0.04. This value is fairly good agreement with those previously found and indicate a pathway for continuing towards the second phase of this methodology which should employ narrowband filters thus creating a full procedure for a long term independent calibration. This next move in this process should be in the near future to be carried on either at IPEN or Howard University/NASA-GSFC Lidar sites depending on operational issues and routine rescheduling in their respective systems.

ACKNOWLEDGMENTS

REFERENCES

[1] Whiteman, D. N., "Examination of the traditional Raman lidar technique. I. Evaluating the temperature-dependent lidar equations," *Applied Optics* **42**(15), 2571–2592 (2003).

[2] Vaughan, G., Wareing, D. P., Thomas, L., and Mitev, V., "Humidity measurements in the free troposphere using raman backscatter," *Quarterly Journal of the Royal Meteorological Society* **114**(484), 1471–1484 (1988).

[3] Penney, C. M. and Lapp, M., "Raman-scattering cross sections for water vapor," *Journal of the Optical Society of America* **66**(5), 422–425 (1976).

[4] Cooney, J. A., "Measurement of the Ratio of the Vibrational Raman Cross Section for H₂O Vapor to the Nitrogen Vibrational-Rotational Raman Band," *Spectroscopy Letters* **3**(11&12), 305–309 (1970).

[5] Sherlock, V., Hauchecorne, A., and Lenoble, J., "Methodology for the independent calibration of raman backscatter water-vapor lida systems," *Applied Optics* **38**, 5816–5837 (1999).

[6] Serikov, I., Froidevaux, M., Ristori, P., Simeonov, V., Arshinov, Y., Bobrovnikov, S., den Bergh, H. V., and Parlange, M. B., "A temperature and water vapor solar-blind Raman lidar: calibration and field tests," in [*Reviewed and revised papers presented at the 24th International Laser Radar Conference,23-28 June 2008, Boulder, Colorado, USA*], Committee of the 24th International Laser Radar Conference, O., ed., Organizing Committee of the 24th International Laser Radar Conference (2008).

[7] Dionisi, D., Congeduti, F., Liberti, G. L., and Cardillo, F., "Automatic calibration procedure for Raman lidar water vapor profiles through not collocated operational radiosoundings," in [*Reviewed and revised papers presented at the 24th International Laser Radar Conference,23-28 June 2008, Boulder, Colorado, USA*], Committee of the 24th International Laser Radar Conference, O., ed., Organizing Committee of the 24th International Laser Radar Conference (2008).

[8] Leblanc, T. and McDermid, I. S., "On the calibration of water vapor Raman lidar and its applicability to the long- term monitoring of atmospheric water vapor," in [*Reviewed and revised papers presented at the 24th International Laser Radar Conference,23-28 June 2008, Boulder, Colorado, USA*], Committee of the 24th International Laser Radar Conference, O., ed., Organizing Committee of the 24th International Laser Radar Conference (2008).

[9] Leblanc, T. and McDermid, I. S., "Accuracy of Raman lidar water vapor calibration and its applicability to long-term measurements," *Applied Optics* **47**, 5592–5603 (2009).

[10] Torres, A. S., Landulfo, E., Whiteman, D. N., and Venable, D., "Water vapor raman lidar independent calibration," in [*Reviewed and revised papers presented at the 24th International Laser Radar Conference,23-28 June 2008, Boulder, Colorado, USA*], Committee of the 24th International Laser Radar Conference, O., ed., Organizing Committee of the 24th International Laser Radar Conference (2008).

[11] Whiteman, D. N., Berkoff, T., Turner, D. D., Tooman, T., Ferrare, R., and Heilman, L., "Water vapor and atmospheric boundary layer temporal evolution in Buenos Aires, Argentina during the night January 1, 2008," in [*ADVANCES IN LASER REMOTE SENSING - SELECTED PAPERS, PRESENTED AT THE 20TH ILRC, VICHY, FRANCE 10 - 14TH JULY 2000*], A. Dabas, C. Loth, J. P., ed., EDITION DE L'ECOLE POLYTECHNIQUE (2000).

[12] Whiteman, D. N., "Examination of the traditional Raman lidar technique. II. Evaluating the ratios for water vapor and aerosols," *Applied Optics* **42**(15), 2593–2608 (2003).

[13] Avila, G., Fernández, J., Tejeda, G., and Montero, S., "The Raman spectra and cross-sections of H_2O, D_2O, and HDO in the OH/OD stretching regions," *Spectroscopy Letters* **3**(11&12), 305–309 (1970).

[14] Measures, R. M., [*Laser Remote Sensing Fundamentals and Applications*], Krieger Publishing Company (1984).

[15] Weitkamp, C., [*Lidar Range-Resolved Optical Remote Sensing of the Atmosphere*], Springer (2005).